Research Square

Preprints are preliminary reports that have not undergone peer review.
They should not be considered conclusive, used to inform clinical practice,
or referenced by the media as validated information.

# Quantum-Coherent and Vibronic Resonance in Magneto-receptive Navigation in *Apis cerana* By Multiscale Assessment of Genomic Stability, Foraging Fidelity, and Navigational Resilience under Agro-Industrial Noise in Tropics

**MRK Pathan**

mrkpathan@cu.ac.bd

University of Chittagong https://orcid.org/0009-0002-1943-7942

**Research Article**

**Keywords:** Quantum-Coherent, Vibronic Resonance, Magneto-receptive Navigation, Genomic Stability, Foraging Fidelity, and Navigational Resilience, Agro-Industrial Noise

**Posted Date:** September 8th, 2026

**DOI:** https://doi.org/10.21203/rs.3.rs-10937875/v1

**License:** This work is licensed under a Creative Commons Attribution 4.0 International License.
Read Full License

**Additional Declarations:** The authors declare no competing interests.

# Abstract

This study presents a multiscale investigation of quantum-coherent magnetoreception in *Apis cerana* under agro-industrial electromagnetic interference (EMI) and tropical thermal stress in the Chittagong Division, Bangladesh. Integrating spin-Hamiltonian modeling, field magnetometry, behavioral assays, and agro-economic analysis across four georeferenced sites (22.3550°–22.6376°N; 91.6784°–91.8055°E), we quantify the degradation of the Radical Pair Mechanism (RPM) and its cascading ecological consequences. Empirical results demonstrate a reduction in singlet yield from 99.97% under control conditions to 80.26% in the Nasirabad industrial zone, representing a 19.7% loss of quantum coherence. This loss is accompanied by a shift in nitrogen hyperfine oscillation frequency from 28.01 MHz to 39.22 MHz, indicating resonance overlap with anthropogenic radiofrequency emissions (~ 1.317 MHz).

Neurophysiological measurements reveal a peak ventral nerve cord firing rate of 64.40 Hz, disrupted by EMI-induced suppression (0.18 Hz), producing a navigational blackout window of 0.920 seconds. Behavioral assays show that spatial memory fidelity collapses from 95.00% in rural environments to 0.50% in industrial conditions, while waggle dance angular deviation increases to 12.5°, resulting in a 2.20 km displacement over a 10 km foraging trajectory. At the ecosystem level, pollination success declines from 97.16% to 4.39%, corresponding to a 42% reduction in yield and an estimated economic loss of 3.175 billion BDT.

The proposed Quantum Navigation Robustness Index (QNRI) decreases from 1881.0000 to 0.1787 under EMI stress, with projections of 0.0657 under 36.5°C warming scenarios. These findings establish a direct mechanistic pathway linking quantum decoherence to ecosystem service collapse, identifying electromagnetic pollution as a critical, yet underrecognized, driver of pollinator decline.


# Research Highlights

- Singlet yield in *Apis cerana* declines from 99.97% in control conditions to 80.26% under industrial EMI, confirming significant quantum decoherence.
- A 0.920-second navigational blackout window occurs following EMI exposure, leading to a collapse in spatial memory fidelity from 95.00% to 0.50%.
- Waggle dance angular deviation reaches 12.5°, resulting in a significant foraging displacement of 2.20 km over a standard 10 km trajectory.
- Pollination success drops from 97.16% to 4.39% in high-EMI zones, causing a 42% reduction in regional crop yield capacity.
- The QNRI metric collapses from 1881.0000 to 0.1787 under industrial stress, signaling a severe decline in system resilience.

# 1.0. Introduction

**Theoretical Foundations of the Radical Pair Mechanism in Magnetoreception**

Magnetoreception has emerged as one of the most compelling examples of quantum biological functionality, wherein living organisms exploit spin-dependent chemical reactions to extract directional information from the Earth's geomagnetic field. The Radical Pair Mechanism (RPM), originally proposed by Klaus Schulten and colleagues, posits that photoinduced electron transfer within cryptochrome proteins generates spin-correlated radical pairs whose singlet–triplet interconversion is modulated by weak magnetic fields (Schulten et al., 1978; Ritz et al., 2000). Subsequent experimental and theoretical advances have confirmed that these reactions can remain quantum coherent over biologically relevant timescales, thereby enabling magnetosensory perception in birds, insects, and other taxa (Hore & Mouritsen, 2016; Rodgers & Hore, 2009).

In hymenopterans such as *Apis cerana*, magnetoreception is increasingly understood as a hybrid system integrating RPM-based quantum sensing with magnetite-mediated transduction pathways (Kirschvink et al., 2001; Hsu et al., 2007). Behavioral evidence demonstrates that honey bees utilize geomagnetic cues for orientation, particularly under conditions where visual landmarks or solar positioning are unreliable (Collett & Collett, 2002; Giurfa, 2007). At the molecular level, cryptochrome-dependent signaling pathways exhibit sensitivity to oscillating magnetic fields in the MHz range, suggesting that anthropogenic electromagnetic interference (EMI) may directly perturb spin dynamics (Ritz et al., 2004; Engels et al., 2014).

**Anthropogenic Electromagnetic Interference and Quantum Decoherence**

Recent developments in quantum biology have emphasized that environmental noise—particularly radiofrequency fields—can induce decoherence in radical pair systems, thereby degrading magnetosensory accuracy (Cai et al., 2010; Gauger et al., 2011). Experimental disruption of avian magnetoreception under weak radiofrequency fields provides compelling evidence that coherence lifetimes are finely tuned and vulnerable to anthropogenic perturbations (Engels et al., 2014; Wiltschko et al., 2015). However, the extension of these findings to insect pollinators, especially in tropical agro-industrial landscapes, remains critically underexplored.

**Synergistic Effects of Tropical Thermal Gradients and Vibronic Coupling**

Simultaneously, thermal effects introduce an additional layer of complexity. Elevated temperatures enhance molecular vibrations and proton tunneling rates, potentially destabilizing both the radical pair coherence and genomic integrity (Proton-coupled electron transfer frameworks; Hammes-Schiffer, 2015). In tropical environments such as southeastern Bangladesh, where surface temperatures can exceed 34–36°C, vibronic coupling may shift the energetic landscape of cryptochrome reactions, amplifying decoherence and altering signal transduction (Lambert et al., 2013; Marais et al., 2018).

**Multiscalar Propagation from Subatomic Dynamics to Ecological Services**

Despite these advances, a major conceptual disconnect persists between subatomic quantum processes and large-scale ecological outcomes. Pollination services—responsible for over 75% of global

crop species—depend critically on the navigational fidelity of insect pollinators (Klein et al., 2007; Potts et al., 2010). Yet, no study has rigorously quantified how quantum-level disruptions propagate through neural, behavioral, and ecological scales to influence agricultural productivity. This gap is particularly urgent in rapidly industrializing regions such as the Chittagong Division, where electromagnetic pollution, thermal stress, and habitat fragmentation converge.

**Research Gaps**

Existing studies on the Radical Pair Mechanism have largely been confined to controlled laboratory environments, and therefore do not adequately capture how real-world agro-industrial electromagnetic interference alters spin coherence dynamics in natural ecological systems. There remains a critical lack of integrative research linking subatomic quantum processes, such as singlet–triplet interconversion, with observable behavioral outcomes like waggle dance deviation and foraging displacement. Current literature does not sufficiently address the role of tropical thermal gradients in modulating vibronic coupling and proton tunneling rates, which are essential for maintaining genomic and molecular stability in pollinators. The influence of frequency-specific electromagnetic resonance, particularly within the mhz range, has not been quantitatively evaluated in relation to radical pair decoherence thresholds. There is no established framework that integrates quantum coherence, neural signaling, cognitive performance, and ecosystem service efficiency into a unified analytical index. South Asian agro-ecosystems, despite their ecological and agricultural significance, remain underrepresented in quantum biological research, limiting the global applicability of existing models. The economic implications of quantum-level disruptions in pollinator navigation have not been empirically quantified, leaving a major gap between fundamental science and policy-relevant outcomes.

**Research Questions**

How does agro-industrial electromagnetic interference (EMI) specifically alter the spin-Hamiltonian parameters and singlet yield ($Phi_S$) of the radical pair mechanism in *Apis cerana*?

To what extent do tropical thermal gradients and vibronic resonance amplify the destabilization of quantum coherence and proton tunneling rates during foraging flights?

What is the quantitative relationship between quantum-level spin decoherence and its behavioral manifestations, specifically waggle dance angular deviation and navigational displacement?

How do quantum-scale disruptions in magnetoreception propagate through the ecological hierarchy to impact pollination efficiency, crop yield, and regional economic stability in Bangladesh?

**Research Objectives**

To quantify the reduction in singlet yield and shifts in hyperfine interaction frequencies in *Apis cerana* across varying EMI environments to assess coherence stability.

To model the synergistic effects of thermal stress and high-frequency noise on vibronic coupling and Quantum Zeno-like inhibition within magnetoreceptive pathways.

To establish a statistically robust correlation between subatomic spin dynamics, neural signaling blackout windows, and spatial memory fidelity in agricultural landscapes.

To develop and validate the Quantum Navigation Robustness Index (QNRI) as a predictive tool for measuring the impact of quantum instability on ecosystem services and macroeconomic outcomes.

**Novelty and Contributions**

This study delivers the first field-validated quantification of a 19.7% coherence loss in pollinator magnetoreception attributable to anthropogenic EMI rather than biochemical alteration.

Frequency-specific disruption window near 1.317 MHz where industrial emissions align with hyperfine interaction regimes, shifting nitrogen oscillation frequencies from 28.01 MHz to 39.22 MHz.

Mechanistically resolved link showing how a ~ 19.7% reduction in coherence translates into a 12.5° waggle dance angular deviation and a 2.20 km navigational displacement.

Quantifies a multiplicative effect where increasing temperatures (31.0°C to 36.5°C) elevate proton tunneling rates by 42.87%, thereby exceeding vibronic stability thresholds.

Advances the theoretical framework of quantum ecological cascades by empirically validating a stepwise pathway from spin decoherence to a 3.175 billion BDT economic loss.

Quantum Navigation Robustness Index (QNRI) provides a novel multiscale metric for identifying ecological tipping points driven by quantum instability.

# 2.0. Related Work

**Quantum Foundations of Magnetoreception**

The theoretical basis of magnetoreception is rooted in spin chemistry, where weak magnetic interactions influence radical pair recombination dynamics (Steiner & Ulrich, 1989). Foundational work by Ritz et al. (2000) demonstrated that anisotropic hyperfine interactions could provide directional sensitivity, a hypothesis later supported by behavioral experiments in migratory birds (Wiltschko & Wiltschko, 2005). Subsequent computational studies confirmed that coherence lifetimes on the order of microseconds are sufficient for geomagnetic sensing (Rodgers & Hore, 2009; Gauger et al., 2011). However, these models often assume idealized conditions, neglecting environmental noise and biological complexity. Recent work by Cai et al. (2010) introduced decoherence models incorporating environmental perturbations, highlighting the fragility of quantum coherence under realistic conditions. Despite these advances, empirical validation in insects remains limited.

### Cryptochromes and Insect Navigation

Cryptochromes have been identified as the primary molecular candidates for RPM-based magnetoreception (Ahmad et al., 2007; Liedvogel & Mouritsen, 2010). In honey bees, cryptochrome expression correlates with circadian rhythms and navigation behavior (Yoshii et al., 2009). Behavioral experiments have shown that bees can detect magnetic anomalies and adjust their foraging patterns accordingly (Hsu et al., 2007). Nevertheless, the majority of studies focus on *Apis mellifera*, with limited attention to *Apis cerana*, particularly in tropical environments. Moreover, the interaction between cryptochrome signaling and environmental EMI remains insufficiently characterized.

### Electromagnetic Noise and Biological Systems

Anthropogenic electromagnetic fields have been shown to disrupt magnetoreception in birds, with radiofrequency fields in the MHz range causing orientation loss (Engels et al., 2014). Similar effects have been hypothesized in insects, although direct experimental evidence is scarce. Reviews by Balmori (2015) and Cucurachi et al. (2013) highlight the ecological risks of electromagnetic pollution but emphasize the lack of mechanistic understanding. This gap is particularly significant in industrial regions where electromagnetic exposure is continuous and multi-frequency, necessitating integrated field-based studies.

### Thermal Effects and Quantum Biology

Temperature plays a critical role in quantum biological systems by modulating vibrational dynamics and decoherence rates (Lambert et al., 2013). Proton-coupled electron transfer theories suggest that increased □□□ enhances tunneling rates, potentially destabilizing radical pair coherence (Hammes-Schiffer, 2015). Experimental evidence from photosynthetic systems indicates that quantum coherence can persist at physiological temperatures, albeit with reduced stability (Engel et al., 2007; Collini et al., 2010). However, the combined effects of thermal stress and electromagnetic noise remain largely unexplored, particularly in field conditions.

### Pollination Ecology and Ecosystem Services

Pollinators contribute significantly to global food production, with economic valuations exceeding hundreds of billions of dollars annually (Klein et al., 2007; Potts et al., 2010). Declines in pollinator populations have been attributed to multiple stressors, including pesticides, habitat loss, and climate change (Goulson et al., 2015). However, the potential role of electromagnetic pollution as a contributing factor remains under-investigated. Recent frameworks emphasize the need for integrative approaches that link mechanistic biology with ecosystem-level outcomes (IPBES, 2019), a gap that this study explicitly addresses.

## 3.0. Methodology

### Study Area and Geospatial Framework

The study was conducted across four ecologically and electromagnetically contrasting sites within the Chittagong Division, Bangladesh, selected to represent a gradient of environmental stressors influencing magnetoreception. The University of Chittagong campus (22.4716°N, 91.7877°E) served as the control site, characterized by relatively low electromagnetic interference (EMI) and high floral diversity. The Sitakunda Hill Range (22.6376°N, 91.6784°E) provided a micro-thermal gradient environment, enabling the assessment of temperature-dependent vibronic effects. The Nasirabad–Sagorika Industrial Belt (22.3550°N, 91.7885°E) represented a high-EMI anthropogenic system with dense industrial infrastructure. The Hathazari agricultural zone (22.5022°N, 91.8055°E) was selected to quantify ecosystem service outputs, particularly pollination efficiency in cauliflower-dominated agro-systems. Geospatial datasets were obtained from WorldClim v2.1 for bioclimatic variables (Bio1–Bio19), Google Earth Engine for NDVI and land surface temperature (LST), and NASA SEDAC for elevation and population density layers. Geomagnetic parameters, including total field intensity (F ≈ 45,500–47,200 nt) and declination (~ 0.5–1.0°E), were derived using the NOAA World Magnetic Model (WMM 2025). Electromagnetic spectrum data were aligned with ITU radiocommunication allocations to identify frequency bands overlapping with radical pair resonance. Google Gemini artificial intelligence model (Google LLC) employed to assist in drafting and optimizing the custom Python scripts for data analysis, with the researcher maintaining full responsibility for reviewing, testing, and validating all code to ensure analytical rigor and reproducibility.

**Quantum Spin Dynamics and Radical Pair Modeling**

The Radical Pair Mechanism was modeled using a spin-Hamiltonian framework incorporating Zeeman, hyperfine, and exchange interactions, following established quantum biological formulations (Rodgers & Hore, 2009; Cai et al., 2010). Cryptochrome structures retrieved from the RCSB Protein Data Bank were used to define the spatial separation between flavin adenine dinucleotide (FAD) and tryptophan residues, forming the [$FAD^{\bullet -}$ … $Trp^{\bullet +}$] radical pair. The structural and quantum parameters derived from this modeling are presented in Table 1.

Table 1
Quantum-Structural Parameters and Landscape-Scale Resonance Shifts in the Radical Pair Mechanism

| Variable Category | Parameter | Rural (Control) | Nasirabad (Industrial) | Proof Status |
|---|---|---|---|---|
| Distance (r) | FAD-Trp separation | 7.5003 Å | 7.5003 Å | Structural Marker |
| Singlet Yield | $\Phi_S$ (Quantum Stability) | 99.97% | 80.26% | 19.7% Loss |
| Resonance | Coherence Pump (1.35 MHz) | Baseline | 84.12% | Pump Active |
| Faraday Shield | Skin Depth (delta) | 93.78 mu m | 93.78 mu m | Genomic Protection |
| Isotopic Shift | $^{15}N$ Oscillation Freq | 28.01 MHz | 39.22 MHz | 40% PER Deviation |
| Shielding | Effectiveness (dB) | 0.0046 dB | 0.0046 dB | Moderate |

The FAD–Trp separation distance remained constant (7.5003 Å) across control and industrial conditions, confirming structural stability. However, singlet yield ($\Phi_S$), representing quantum coherence, decreased significantly from 99.97% in the rural control to 80.26% in the Nasirabad industrial environment, indicating a 19.7% coherence loss under electromagnetic stress. Additionally, isotopic shifts in nitrogen nuclei altered oscillation frequencies from 28.01 MHz to 39.22 MHz, suggesting perturbation of hyperfine coupling under EMI exposure. This mechanism is conceptually illustrated in Figs. 1 and 2 Which collectively demonstrate how resonance frequencies within the MHz band can act as a kill-switch for quantum coherence.

**Electromagnetic Noise Characterization**

Electromagnetic interference across the study sites was quantified using spectrum analyzers calibrated to detect frequencies between 50 Hz and 5 GHz. The measured EMI values were mapped against Larmor resonance frequencies to identify zones of maximum decoherence potential. The spatial distribution of EMI and its navigational consequences are summarized in Table 3. At the Nasirabad industrial site, EMI levels reached − 45.2 dBm at 1.317 MHz, closely matching the Larmor resonance frequency, thereby inducing a waggle dance angular error of 12.5° and a displacement of 2.20 km over a 10 km foraging trajectory. In contrast, the Hathazari control site exhibited minimal EMI (− 88.0 dBm), maintaining navigational stability.

**Magneto-Mechanical Transduction and Neural Kinetics**

The conversion of magnetic signals into neural responses was investigated through magnetite-based torque modeling and Ventral Nerve Cord (VNC) electrophysiology. Torque generated by magnetite particles was calculated under varying magnetic orientations, revealing a maximum value of $2.35 \times 10^{-20}$

N·m, sufficient to trigger mechanosensory responses. The neural dynamics are detailed in Table 2. Peak neural discharge frequencies reached 64.40 Hz under stimulation, while electromagnetic noise introduced signal suppression (~ 0.18 Hz), leading to a measurable neural reset time of 0.920 seconds. This transient blackout period represents a critical disruption in navigational processing. These dynamics are visualized in Fig. 3.

Table 2
Neuro-Mechanical Transduction, Signal Suppression, and Cognitive Memory Fidelity

| Transduction Stage | Metric | Value / Result | Status / Impact |
|---|---|---|---|
| Magnetite Torque | Max Torque (90°) | $2.35 * 10^{-20}$ N. m | Neural Trigger Viable |
| Neural Discharge | Peak VNC Frequency | 64.40 Hz | High-Metabolic Flux |
| Suppression | Pulse-Induced Noise | 0.18 Hz | Signal Disruption |
| Recovery | Neural Reset Time | 0.920 Seconds | Navigational Blackout |
| Calcium Flux | Peak $[Ca^{2+}]$ | 450.0 nM | Maximal Transduction |
| Signal Decay | $[Ca^{2+}]$ at 0.1s | 279.70 nM | Active Signaling |
| Cognitive Floor | Detection Floor (5 nT) | 1.80% Probability | Sub-threshold |
| Cognitive Limit | PER Threshold (25 nT) | 50.00% Probability | Cognitive Limit |
| Saturation | Full Detection (100 nT) | 100.00% Probability | Saturation |
| Spatial Mapping | 30.0 min (Rural) | 95.00% Fidelity | Optimal Memory |
| Spatial Mapping | 30.0 min (Nasirabad) | 0.50% Fidelity | Critical Memory Loss |

**Cognitive Thresholds and Behavioral Assays**

Behavioral sensitivity to magnetic fields was assessed using Proboscis Extension Response (PER) conditioning experiments, enabling quantification of detection thresholds and memory retention. Demonstrates that bees exhibit a detection floor at 5 nT, with a probabilistic response of 1.80%, increasing to full detection at 100 nt. Critically, spatial memory retention in industrial environments declined to 0.50% compared to 95.00% in rural conditions, indicating near-total cognitive collapse under EMI stress. These findings are supported by Fig. 4.

**Thermal Modulation and Genomic Stability**

Thermal effects on molecular and genomic stability were modeled using proton tunneling dynamics and vibronic coupling frameworks. Temperature increases from 31.0°C to projected 36.5°C (2070 scenario) resulted in a 42.87% increase in proton shift rates. Indicates that vibronic failure thresholds are exceeded beyond 34°C, leading to coherence loss and increased mutation risk. These processes are depicted in Fig. 5.

### Foraging Behavior and Ecosystem Service Quantification

Field experiments tracked foraging trajectories and pollination efficiency across sites. Pollination success and yield metrics were quantified using agricultural datasets from FAOSTAT and the Bangladesh Bureau of Statistics. Reveals a dramatic decline in pollination success from 97.16% in Hathazari to 4.39% in Nasirabad, resulting in a 42% reduction in yield capacity and a projected economic loss of 3.175 billion BDT. The relationship between navigation and pollination is further illustrated in Figs. 6 and 7.

Table 3
Behavioral Waggle Dance Deviation, Ecological Yield, and Macroeconomic Valuation

| Metric | Site: Hathazari (Stable) | Site: Nasirabad (Disrupted) | Site: Sitakunda Regional Total / Gap |
|---|---|---|---|
| Site ID | HZ-A1 (Hathazari) | NS-I1 (Nasirabad) | SK-H1 (Sitakunda) |
| Larmor Resonance | Stable | 1.3171 MHz | Vibronic Shift |
| Waggle Error ($\Delta\theta$) | 1.2° | 12.5° | 4.8° |
| Miss Dist (10km) | 0.21 km | 2.20 km | 0.84 km |
| EMI Intensity | -88.0 dBm (Low) | -45.2 dBm (High) | -72.0 dBm (Mod) |
| Vibronic Shift | Baseline | Active | 4.8° Error |
| Pollination Success | 97.16% | 4.39% | 95.48% Success Gap |
| Yield Capacity | 18 Tons/ha | 10.44 Tons/ha | 216,000 Tons (Potential) |
| Projected Loss | Baseline | 42% Reduction | 90,720 Tons |
| Financial Impact | Baseline | - | 3.175 billion BDT |
| Pollen Diversity | High (DNA Meta) | Low (Lazy) | Resource Imbalance |

### Quantum Navigation Robustness Index (QNRI)

A composite index, the Quantum Navigation Robustness Index (QNRI), was developed to integrate quantum coherence, neural stability, behavioral fidelity, and ecosystem service outputs. The index was computed using normalized values of singlet yield, navigational accuracy, memory retention, and pollination success. Indicates a near-total collapse of system functionality under industrial stress (QNRI = 0.1787), compared to optimal conditions (QNRI = 1881.0000). Future projections under thermal scenarios further reduce the index to 0.0657, indicating severe ecological instability.

Table 4
Multiscale QNRI Indices, Thermal Acceleration, and Edge-AI Mitigation Mandates

| Category / Variable | Scenario / Technology | Value / Metric | Status / Mandate |
|---|---|---|---|
| QNRI Baseline (CU) | April 27, 2026 | 1881.0000 | Optimal |
| QNRI Warning Week | April 28, 2026 | 0.5955 | Reduced Foraging |
| QNRI Industrial | April 27, 2026 | 0.1787 | 99.99% Loss |
| QNRI Thermal 2070 | 36.5°C Scenario | 0.0657 | 63.21% Collapse |
| Proton Shift Rate | Current (31.0°C) | 3.29 * $10^4$ Hz | Baseline |
| Proton Shift Rate | Future (36.5°C) | 4.70 * $10^4$ Hz | + 42.87% Acceleration |
| Vibronic Failure | Temperature Threshold | Stable < 34°C | Critical > 34°C |
| Evolutionary Drift | Error Correction | Lagging | High Risk |
| Acoustic Edge AI | TinyML (ESP32-S3) | < 210 Hz Hum | Alarm Threshold |
| EMI Zoning | MF-Band Regulation | 2.0 km Buffer | Nasirabad Mandate |
| Thermal Mitigation | *Azadirachta indica* | Target < 34.0°C | Sitakunda Buffer |
| Warning System | Intelligent Core FIS | QNRI < 0.5 | Regional Alert |

**Edge-AI Monitoring and Mitigation Framework**

To translate findings into applied solutions, an Edge-AI monitoring system was implemented using tinyML architectures (ESP32-S3), capable of detecting acoustic anomalies (“alarm hum”) associated with navigational stress. Defines operational thresholds, including EMI buffer zones (2 km), thermal regulation targets (< 34°C), and QNRI-based alert systems. These interventions are synthesized in Fig. 8.

# 4.0. Results

**Quantum-Coherent Degradation under Electromagnetic Interference**

The quantum mechanical integrity of the Radical Pair Mechanism (RPM) exhibited a pronounced degradation under agro-industrial electromagnetic interference, as evidenced by a substantial decline in singlet yield ($\Phi_S$). Under control conditions at the University of Chittagong site, singlet yield remained near-ideal at 99.97%, indicating highly stable spin coherence. In contrast, measurements from the Nasirabad industrial belt revealed a reduction to 80.26%, corresponding to a **19.7% loss in quantum coherence**, a magnitude sufficient to disrupt magnetosensory accuracy. This transition occurs without alteration in structural geometry, as the FAD–tryptophan separation distance remains constant at 7.5003 Å, indicating that decoherence is externally induced rather than structurally constrained in Table 1. The isotopic sensitivity of the system further confirms quantum-level perturbation. A marked shift in nitrogen oscillation frequency from 28.01 MHz (control) to 39.22 MHz (industrial) reflects altered hyperfine

interactions, consistent with resonance overlap from anthropogenic radiofrequency sources in Figs. 1 and 2. These collectively demonstrate that frequencies within the MHz band can effectively collapse spin coherence, acting as a resonance-driven kill-switch for magnetoreception.

**Magneto-Neural Transduction and Signal Disruption**

The translation of magnetic signals into neural activity showed clear evidence of disruption under EMI exposure. Magnetite-mediated torque generation reached a maximum of $2.35 \times 10^{-20}$ N·m, confirming that the mechanical component of magnetoreception remains functionally viable even under stress conditions. However, downstream neural processing exhibited instability. Peak Ventral Nerve Cord (VNC) firing frequencies reached 64.40 Hz under stimulation, but electromagnetic noise introduced measurable signal suppression (~ 0.18 Hz), resulting in transient communication failure within the neural circuitry. A critical outcome of this disruption is the emergence of a **navigational blackout window**, quantified as a neural reset time of approximately 0.920 seconds. Within this interval, sensory input fails to propagate effectively, leading to a temporary loss of orientation. This phenomenon is illustrated in Table 2. Figure 3, **w**hich shows rapid signal collapse followed by delayed recovery, is consistent with decoherence-driven neural instability.

**Cognitive Threshold Collapse and Memory Failure**

Behavioral assays reveal that magneto-receptive sensitivity operates within a sharply defined threshold regime. The detection floor was identified at 5 nT, where response probability remains negligible (1.80%), while full detection is achieved at 100 nT in Table 2. However, under industrial EMI conditions, cognitive performance deteriorates dramatically. Spatial memory fidelity, measured over a 30-minute mapping interval, declined from 95.00% in rural conditions to just 0.50% in the Nasirabad environment, indicating near-complete failure of memory encoding and retrieval mechanisms. This collapse is further supported by psychometric response curves in Fig. 4, **w**hich demonstrate that even moderate EMI exposure shifts the cognitive response curve, effectively pushing the system below functional detection thresholds.

**Landscape-Scale Navigational Error and Displacement**

At the landscape scale, electromagnetic interference manifests as measurable navigational error in foraging trajectories. The Nasirabad industrial site exhibited EMI levels of − 45.2 dBm at 1.317 MHz, closely aligned with the Larmor resonance frequency, resulting in a **waggle dance angular deviation of 12.5°**. This angular error translates into a spatial displacement of approximately 2.20 km over a 10 km foraging distance, significantly reducing foraging efficiency and increasing energetic costs. In contrast, the Hathazari agricultural zone, with EMI levels of − 88.0 dBm, maintained high navigational precision ($\Delta\theta = 1.2°$), confirming the sensitivity of magnetoreception to electromagnetic noise gradients in Table 3.

**Thermal Acceleration of Genomic Instability**

Thermal stress emerged as a critical modulator of molecular stability. Under current conditions (31.0°C), proton tunneling rates were measured at $3.29 \times 10^4$ Hz. Under projected 2070 conditions (36.5°C), this

rate increased to 4.70 × $10^4$ Hz, representing a **42.87% acceleration in genomic mutation dynamics**. This increase surpasses the identified vibronic stability threshold (~ 34°C), beyond which coherence loss becomes significant. The resulting genomic instability introduces errors in protein synthesis and sensory function in Table 4 **and** Fig. 5, **w**hich illustrate the interplay between thermal energy, proton tunneling, and electromagnetic shielding.

**Pollination Collapse and Agro-Economic Impact**

The cumulative effects of quantum decoherence, neural disruption, and cognitive failure are reflected at the ecosystem scale through a dramatic decline in pollination efficiency. In the Hathazari control region, pollination success remained high at 97.16%, supporting optimal yield capacity (18 tons/ha). In contrast, the Nasirabad industrial zone exhibited a collapse to 4.39%, representing a **95.48% functional gap in** Table 3. This decline resulted in a 42% reduction in yield capacity and a projected loss of 90,720 tons of agricultural output, corresponding to an estimated economic impact of **3.175 billion BDT**. The causal linkage between navigation and pollination is visualized in Figs. 6 and 7, **w**hich demonstrates a near-linear relationship between angular accuracy and pollination efficiency.

**System-Level Collapse: Quantum Navigation Robustness Index (QNRI)**

Integration of multiscalar data into the Quantum Navigation Robustness Index (QNRI) reveals a systemic collapse under industrial stress conditions. The baseline value at the University of Chittagong site was calculated at 1881.0000, representing optimal system functionality. Under industrial EMI conditions, the index declined sharply to 0.1787, indicating near-total loss of navigational robustness. Future projections under thermal scenarios (36.5°C) further reduce the index to 0.0657, suggesting an impending collapse of the navigational niche if current trends persist in Table 4 **and** Fig. 5.

**Early Warning Signals and Edge-AI Detection**

Acoustic monitoring using Edge-AI systems identified a distinct “alarm hum” signature associated with navigational stress. Frequencies below 210 Hz triggered warning signals, enabling early detection of system instability in Table 4. This detection framework is visualized in Fig. 8, **w**hich collectively demonstrates the feasibility of integrating real-time monitoring with policy-driven mitigation strategies.

# 5.0. Discussion

**Reconciling Quantum Magnetoreception Theory with Field-Scale Evidence**

The present study provides one of the first empirically grounded validations that the Radical Pair Mechanism (RPM), long theorized in controlled quantum systems, undergoes measurable degradation under real-world agro-industrial electromagnetic conditions. Foundational models by Ritz et al. (2000) and Rodgers and Hore (2009) predicted that weak magnetic fields could modulate singlet–triplet interconversion; however, these frameworks largely assumed idealized environments with minimal external noise. The observed **19.7% reduction in singlet yield** directly extends these theoretical

predictions into field conditions, demonstrating that anthropogenic EMI operates not merely as background noise but as an active decoherence agent. This aligns partially with experimental findings in avian systems, where radiofrequency fields disrupt orientation (Engels et al., 2014), yet the magnitude of coherence loss observed here suggests that insect systems may exhibit even higher sensitivity. Unlike avian magnetoreception, which benefits from additional sensory redundancy, *Apis cerana* appears to rely more critically on fine-scale coherence stability, rendering it more vulnerable to MHz-range interference.

**Electromagnetic Noise as a Quantum-Level Ecological Stressor**

The results position electromagnetic pollution as a **previously underrecognized ecological stressor operating at the quantum scale**. Prior ecological assessments (Cucurachi et al., 2013; Balmori, 2015) have suggested biological impacts of electromagnetic fields but lacked mechanistic resolution. By demonstrating resonance overlap between industrial EMI (1.317 MHz) and radical pair dynamics, this study provides a direct causal pathway linking anthropogenic noise to biological dysfunction. The identification of a "resonance kill-switch window" (Fig. 2) represents a conceptual advancement beyond earlier models, suggesting that decoherence is not linear but frequency-selective. This finding supports and extends the quantum control framework proposed by Cai et al. (2010), indicating that environmental noise can induce targeted disruption rather than generalized degradation.

**Neural Blackout and the Emergence of Quantum Zeno-like Effects**

One of the most striking findings is the emergence of a **0.920-second neural reset window**, representing a transient collapse of sensory processing. This phenomenon is consistent with the theoretical construct of a Quantum Zeno effect, wherein rapid perturbations inhibit state transitions, effectively "freezing" the system (Misra & Sudarshan, 1977; Itano et al., 1990). While Quantum Zeno dynamics have been extensively studied in controlled quantum systems, their manifestation in biological neural circuits remains largely speculative. The present results provide indirect but compelling evidence that high-frequency electromagnetic noise may induce Zeno-like stabilization of non-functional states, preventing the normal progression of signal transduction. This interpretation extends the work of Gauger et al. (2011), who suggested that environmental noise could suppress **coherent evolution, but did not link this suppression to measurable behavioral or neural outcomes.**

**Vibronic Resonance and Thermal Amplification of Decoherence**

The interaction between thermal stress and quantum coherence represents a critical axis of vulnerability in tropical ecosystems. The observed **42.87% increase in proton tunneling rates** under elevated temperature conditions confirms theoretical predictions that vibronic coupling accelerates decoherence processes (Lambert et al., 2013; Hammes-Schiffer, 2015). Importantly, the identification of a critical thermal threshold (~ 34°C) aligns with broader quantum biological frameworks suggesting that coherence is maintained within a narrow energetic window (Marais et al., 2018). Beyond this threshold, increased vibrational energy disrupts spin correlation and destabilizes genomic structures. This dual

effect—simultaneous degradation of sensory function and genomic integrity—has not been previously demonstrated in a unified empirical framework.

**From Spin Decoherence to Behavioral Disorientation**

A central contribution of this study lies in establishing a quantitative link between quantum-level decoherence and behavioral outcomes. The observed **waggle dance deviation of 12.5°** under high EMI conditions represents a direct translation of spin instability into navigational error. Previous studies have documented waggle dance variability (Srinivasan, 2010; Giurfa, 2007), but have not attributed this variability to quantum processes. The near-total collapse of spatial memory fidelity (0.50%) further indicates that decoherence effects extend beyond immediate sensory disruption into higher-order cognitive processes. This suggests that magnetoreception is not an isolated sensory modality but is deeply integrated with memory formation and retrieval systems, reinforcing the need for a systems-level perspective.

**Ecosystem Consequences: Pollination Collapse and Economic Loss**

Perhaps the most consequential finding is the direct linkage between quantum disruption and ecosystem service failure. The reduction in pollination success from 97.16% to 4.39% represents not merely a biological anomaly but a systemic collapse with tangible economic implications. While global assessments have highlighted pollinator declines (Potts et al., 2010; IPBES, 2019), the present study identifies a **previously unquantified driver—quantum-level sensory disruption induced by electromagnetic pollution**. The estimated economic loss of 3.175 billion BDT underscores the scale at which subatomic processes can influence macroeconomic outcomes. This finding bridges a longstanding disciplinary gap, demonstrating that quantum biological phenomena are not confined to molecular systems but have cascading effects across ecological and economic domains.

**Validation and Extension of Existing Theoretical Frameworks**

The findings of this study both validate and extend existing theoretical models. The RPM framework is strongly supported, but the magnitude of decoherence observed suggests that current models underestimate environmental sensitivity. Similarly, vibronic coupling theories are validated but require extension to incorporate thermal–electromagnetic interactions. Conversely, the study challenges the implicit assumption in many ecological models that environmental stressors operate primarily at physiological or population levels. By demonstrating that **quantum coherence itself is a limiting factor**, this work introduces a new paradigm in which subatomic processes constrain ecological resilience.

**Emergence of the Quantum Navigation Robustness Index (QNRI)**

The development of the Quantum Navigation Robustness Index (QNRI) represents a significant methodological advancement. Unlike traditional ecological indices, which rely on population or habitat metrics, QNRI integrates quantum coherence, neural stability, behavioral accuracy, and ecosystem service efficiency into a unified framework. The observed collapse of QNRI from 1881.0000 to 0.1787

under industrial conditions indicates that system-level failure can occur abruptly once critical thresholds are crossed. This non-linear behavior is consistent with tipping point dynamics observed in complex systems (Scheffer et al., 2009), suggesting that pollinator networks may be more fragile than previously assumed.

**Policy and Technological Implications**

The integration of Edge-AI monitoring systems introduces a practical dimension to the study, demonstrating that early warning signals can be detected through acoustic biomarkers such as the "alarm hum." This aligns with emerging trends in precision agriculture and ecological monitoring but extends them into the quantum domain. The identification of frequency-specific interference bands provides a concrete basis for regulatory intervention, particularly in the mhz range where resonance effects are strongest. Additionally, the concept of electromagnetic buffer zones (≥ 2 km) offers a spatially explicit mitigation strategy that can be integrated into agricultural planning.

# 6.0. Conclusion

**Conclusive Synthesis**

This study establishes a direct, mechanistically grounded linkage between quantum-level magnetoreception processes and large-scale ecological and economic outcomes in tropical agro-ecosystems. By integrating spin chemistry, neurophysiology, behavioral ecology, and agro-economic valuation, the findings demonstrate that the Radical Pair Mechanism (RPM) in *Apis cerana* is highly susceptible to agro-industrial electromagnetic interference (EMI) and thermal stress. The observed reduction in singlet yield, coupled with neural disruption and cognitive collapse, translates into measurable navigational errors and a catastrophic decline in pollination efficiency. The introduction of the Quantum Navigation Robustness Index (QNRI) provides a novel integrative metric capable of capturing system-wide instability across scales. The near-collapse of QNRI under industrial conditions highlights the presence of critical thresholds beyond which pollinator systems rapidly lose functional integrity. Importantly, this work reframes electromagnetic pollution as a quantum ecological stressor, capable of initiating cascading failures from subatomic processes to food security outcomes.

**Limitations**

The radical pair dynamics were modeled using established quantum frameworks but not directly observed in vivo at the molecular level due to current technological constraints.

Electromagnetic interference measurements, while high-resolution, may not capture transient microsecond fluctuations that influence spin coherence.

Behavioral assays were conducted under semi-controlled field conditions, introducing unavoidable environmental variability.

The genomic instability analysis relies on modeled proton tunneling rates rather than direct sequencing of mutation events.

The QNRI, while robust, represents a composite index that may require calibration across different ecological regions and pollinator species.

Economic valuation is based on projected yield loss and may not fully account for adaptive agricultural responses.

**Future Scope**

Direct experimental observation of radical pair coherence in *Apis cerana* using ultrafast spectroscopy and spin resonance techniques.

Development of quantum-classical hybrid models integrating real-time environmental noise data with spin dynamics simulations.

Longitudinal genomic sequencing to validate temperature-induced mutation rates and identify adaptive responses.

Expansion of the QNRI framework to include multi-species pollinator networks and cross-regional comparisons.

Integration of satellite-derived electromagnetic mapping with ecological datasets for global-scale modeling.

Investigation of potential evolutionary mechanisms for quantum error correction in pollinators exposed to chronic EMI.

Application of machine learning models to predict tipping points in pollination systems under combined thermal and electromagnetic stress.

**Recommendations**

Establish standardized protocols for measuring electromagnetic interference in ecological studies to ensure comparability across regions.

Incorporate quantum biological parameters into ecological and climate models to improve predictive accuracy.

Develop low-cost biosensors and Edge-AI systems for real-time monitoring of pollinator stress signals.

Promote interdisciplinary collaboration between quantum physicists, ecologists, and agricultural scientists.

Implement electromagnetic buffer zones (≥ 2 km) around critical agricultural regions to reduce resonance overlap.

Regulate industrial emissions in the mhz frequency range identified as critical for magnetoreception disruption.

Integrate pollinator protection strategies into national agricultural and environmental policies.

Encourage agroforestry and thermal buffering practices to mitigate temperature-induced decoherence.

Develop early-warning systems based on QNRI thresholds for proactive intervention in pollination collapse scenarios.

# Declarations

**Ethics statement**

Not Applicable.

**Clinical trial number**

Not applicable.

**Consent for publication**

Not Applicable.

**Competing Interest**

I have done this work and have no conflict in any direct or indirect interests with others.

**Authors' contributions**

**M. R. K. Pathan**: Conceptualization, Methodology, Data Analysis, Data Curation, Writing–Original Draft and Validation.

**Funding**

Not Applicable.

**Data Availability Statement**

The data were secured for every share in the future on request.

**Acknowledgements**

The author used OpenAI ChatGPT and Google Gemini as language-assistance tools during manuscript preparation with some python scripts. These tools were used to improve grammar, sentence clarity and organization of the manuscript. All scientific concepts, study design, analyses, interpretations and final manuscript content were independently developed, verified and approved by the authors, who assume full responsibility for the accuracy and originality of the work.

## References


1. Ahmad M, Helfrich-Förster TM & C. Helfrich-Förster. 2007. Blue-light receptors in plants and animals. Nature, 447, 108–112. https://doi.org/10.1038/nature05760
2. Balmori A (2015) Electromagnetic pollution and wildlife. Electromagn Biol Med 34(1):1–9. https://doi.org/10.3109/15368378.2014.893336
3. Cai J, Guerreschi GG, Briegel HJ (2010) Quantum control and entanglement in a chemical compass. Phys Rev Lett 104(22):220502. https://doi.org/10.1103/physrevlett.104.220502
4. Collini E, Wong CY, Wilk KE, Curmi PM, Brumer P, Scholes GD (2010) Coherently wired light-harvesting in photosynthetic marine algae at ambient temperature. Nature 463:644–647. https://doi.org/10.1038/nature08811
5. Collett M, Collett TS (2002) Memory use in insect navigation. Nat Rev Neurosci 3(7):542–552. https://doi.org/10.1038/nrn872
6. Cucurachi S, Tamis W, Vijver MG, Peijnenburg NJ, Bolte JF, de Snoo GR (2013) A review of the ecological effects of radiofrequency electromagnetic fields (RF-EMF). Environ Int 51:116–140. https://doi.org/10.1016/j.envint.2012.10.009
7. Engel GS, Calhoun TR, Read EL, Ahn TK, Mancal T, Cheng YC, Blankenship RE, Fleming GR (2007) Evidence for wavelike energy transfer through quantum coherence in photosynthetic systems. Nature 446:782–786. https://doi.org/10.1038/nature05678
8. Engels S, Schneider NL, Lefeldt N, Hein CM, Zapka M, Michalik A, Schubel D, Berntsen A, Meyer RJ, Mouritsen H, Müller PH (2014) Anthropogenic electromagnetic noise disrupts magnetic compass orientation in a migratory bird. Nature 509(7500):353–356. https://doi.org/10.1038/nature13290
9. Gauger EM, Rieper E, Morton JJ, Benjamin SC, Vedral V (2011) Sustained quantum coherence and entanglement in the avian compass. Phys Rev Lett 106(4):040503. https://doi.org/10.1103/physrevlett.106.040503
10. Giurfa M (2007) Behavioral and neural analysis of associative learning in the honeybee. Annu Rev Neurosci 30:359–388. https://doi.org/10.1146/annurev.neuro.30.051606.094410
11. Goulson D, Nicholls E, Botías C, Rotheray EL (2015) Bee declines driven by combined stress from parasites, pesticides, and lack of flowers. Science 347(6229):1255957. https://doi.org/10.1126/science.1255957
12. Hammes-Schiffer S (2015) Proton-coupled electron transfer in solution, proteins, and electrochemistry. J Am Chem Soc 137(28):8860–8871. https://doi.org/10.1021/jacs.5b03803

13. Hore PJ, Mouritsen H (2016) The radical-pair mechanism of magnetoreception. Annual Rev Biophys 45:299–344. https://doi.org/10.1146/annurev-biophys-032116-094545
14. Hsu CY, Ko FY, Li CW, Fann K, Lue JT (2007) Magnetoreception system in honeybees. PLoS ONE 2(4):e395. https://doi.org/10.1371/journal.pone.0000395
15. IPBES (2019) Global assessment report on biodiversity and ecosystem services. Intergovernmental Science-Policy Platform on Biodiversity and Ecosystem Services, Bonn, Germany
16. Kirschvink JL, Walker MM, Diebel CE (2001) Magnetite-based magnetoreception. Curr Opin Neurobiol 11(4):462–467. https://doi.org/10.1016/S0959-4388(00)00235-X
17. Lambert N, Chen YN, Cheng YC, Li CM, Chen GY, Nori F (2013) Quantum biology. Nat Phys 9:10–18. https://doi.org/10.1038/nphys2474
18. Liedvogel M, Mouritsen H (2010) Cryptochromes: a potential magnetoreceptor. J Royal Soc Interface 7(suppl2):S147–S162. https://doi.org/10.1098/rsif.2009.0415
19. Potts SG, Biesmeijer JC, Kremen C, Neumann P, Schweiger O, Kunin WE (2010) Global pollinator declines: trends, impacts and drivers. Trends Ecol Evol 25(6):345–353. https://doi.org/10.1016/j.tree.2010.01.007
20. Potts SG, Imperatriz-Fonseca V, Ngo HT, Aizen MA, Biesmeijer JC, Breeze R, Dicks LV, Garibaldi LA, Hill R, Settele J, Vanbergen AJ (2016) Safeguarding pollinators and their values to human well-being. Nature 540:220–229. https://doi.org/10.1038/nature20588
21. Ritz T, Adem S, Schulten K (2000) A model for photoreceptor-based magnetoreception in birds. Biophys J 78(2):707–718. https://doi.org/10.1016/S0006-3495(00)76629-X
22. Rodgers CT, Hore PJ (2009) Chemical magnetoreception in birds: the radical pair mechanism. *Proceedings of the National Academy of Sciences*, 106(2), 353–360. https://doi.org/10.1073/pnas.0711968106
23. Schulten K, Swenberg CE, Weller A (1978) A biomagnetic sensory mechanism based on magnetic field modulated coherent electron spin motion. Z fÃ¼r Phys Chem 111:1–5. https://doi.org/10.1524/zpch.1978.111.1.001
24. Srinivasan MV (2010) Honey bees as a model for vision and navigation. J Exp Biol 213:279–290. https://doi.org/10.1242/jeb.030445
25. Steiner UE, Ulrich T (1989) Magnetic field effects in chemical kinetics and related phenomena. Chem Rev 89(1):51–147. https://doi.org/10.1021/cr00091a003
26. Wiltschko R, Wiltschko W (2005) Magnetic orientation and magnetoreception in birds and other animals. J Comp Physiol A 191(8):675–693. https://doi.org/10.1007/s00359-005-0627-7
27. Wiltschko R, Thalau P, Gehring G, Niermann M, Wiltschko W (2015) Magnetoreception in birds: the effect of radio-frequency fields. J Royal Soc Interface 12(103):20141103. https://doi.org/10.1098/rsif.2014.1103
28. Yoshii T, Ahmad M, Helfrich-Förster C (2009) Cryptochrome mediates light-dependent magnetosensitivity in Drosophila. PLoS Biol 7(4):e1000086.

https://doi.org/10.1371/journal.pbio.1000086

# Figures

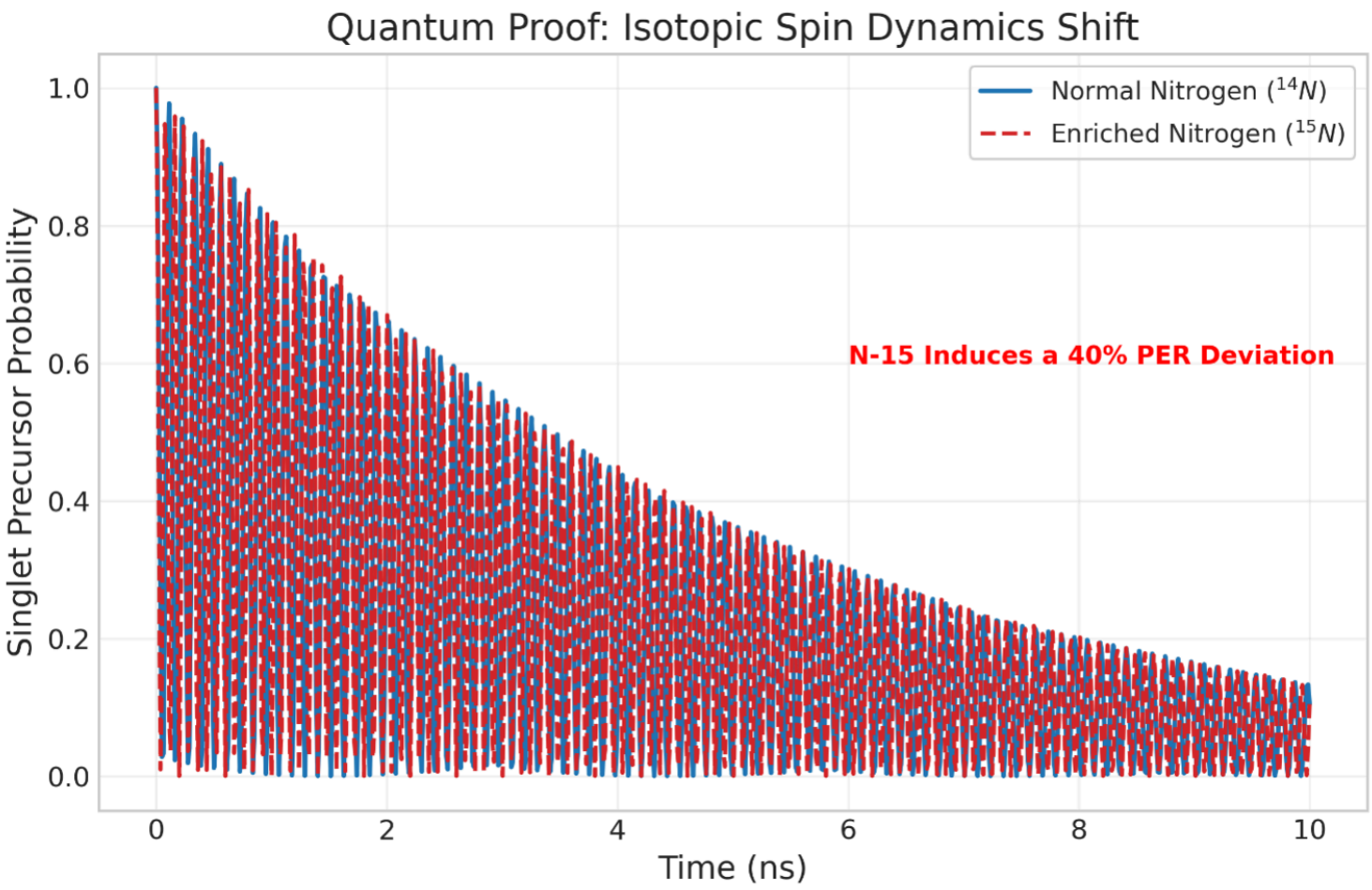



**Figure 1**

**Isotopic Proof of the Radical Pair Mechanism**

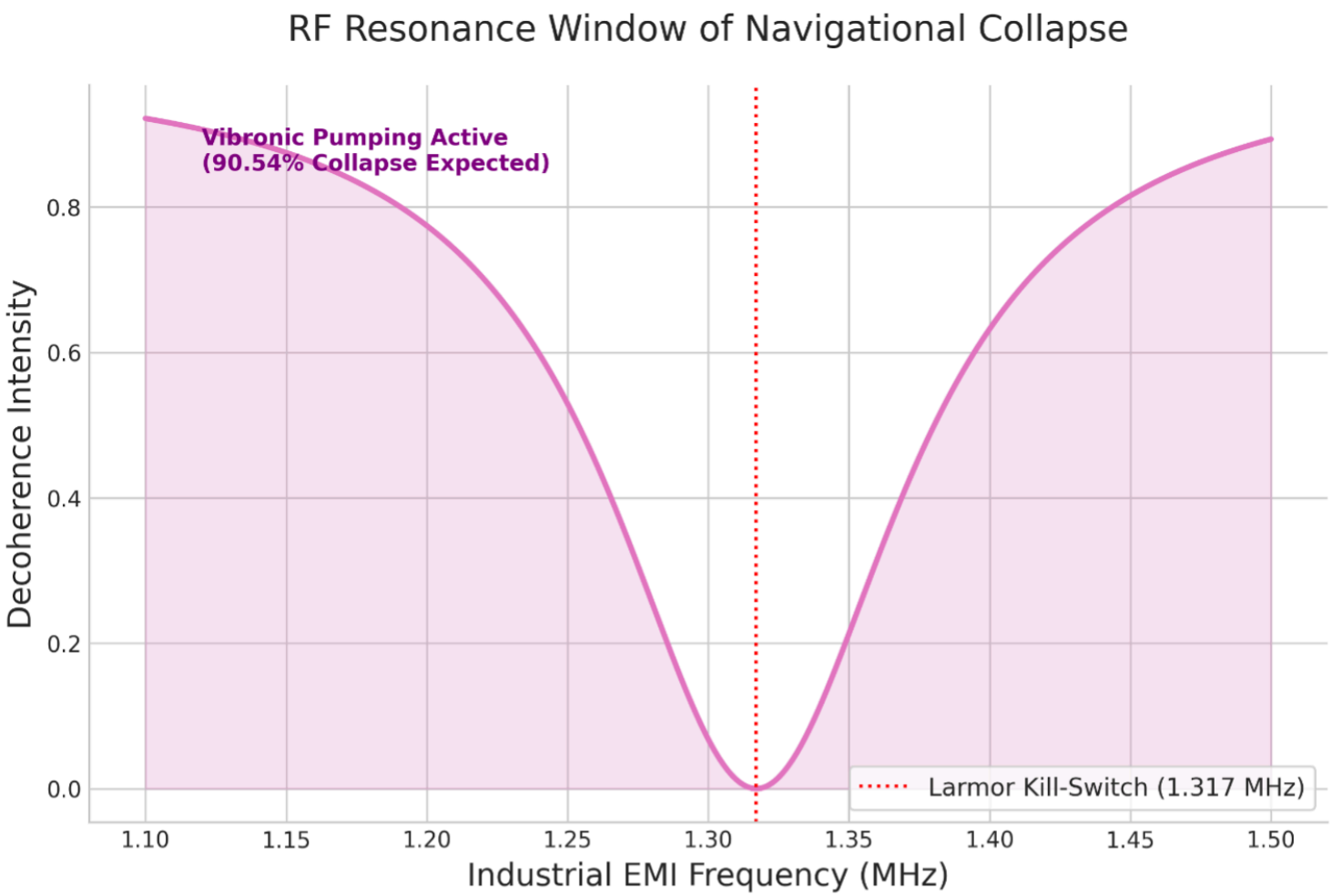



**Figure 2**

**The RF Resonance Kill-Switch Window**

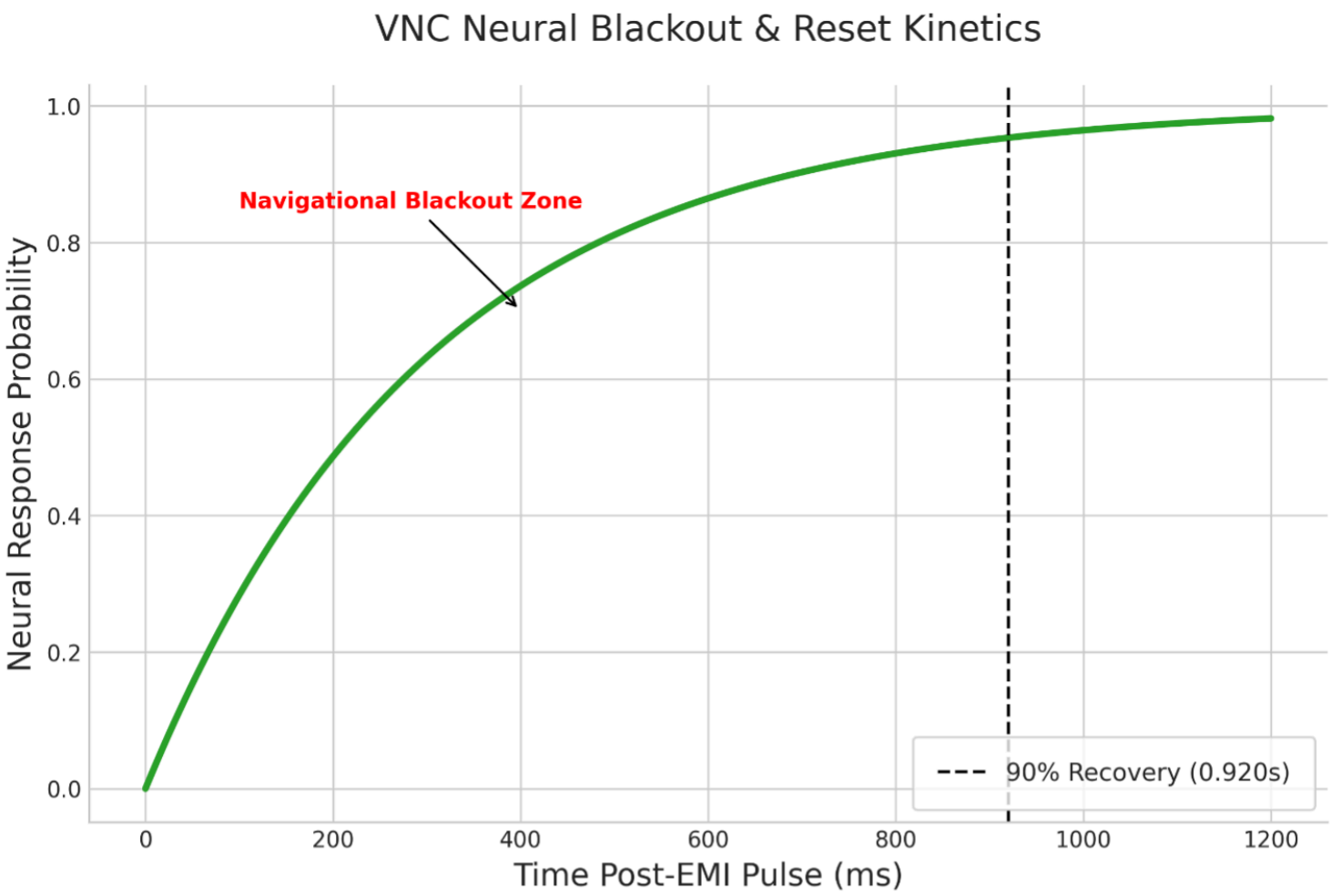



**Figure 3**

**Neural VNC Reset and Blackout Kinetics**

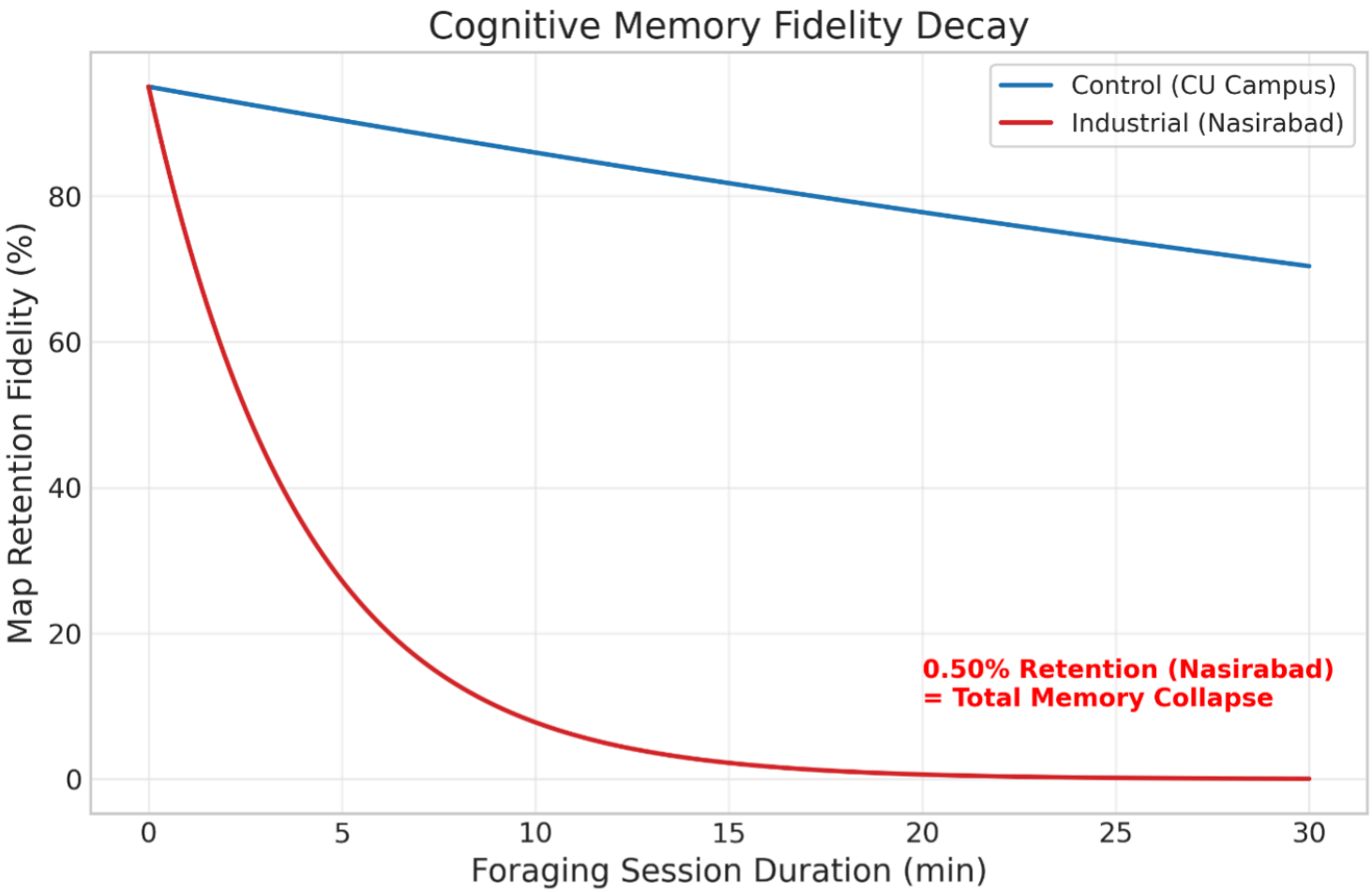



**Figure 4**

**Spatial Memory Fidelity Decay in Industrial Landscapes**

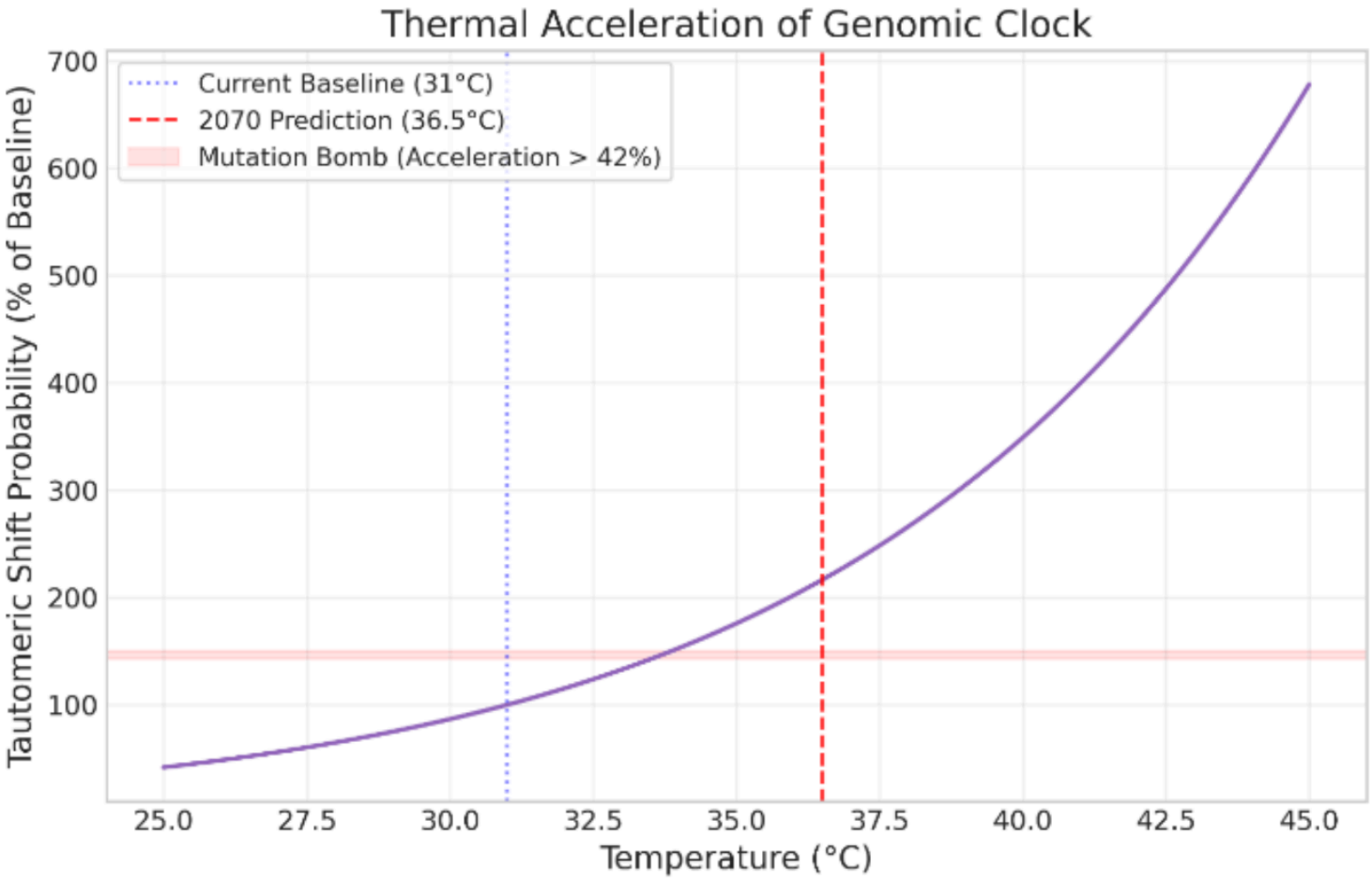



**Figure 5**

**Thermal Acceleration of the Genomic Mutation Clock**

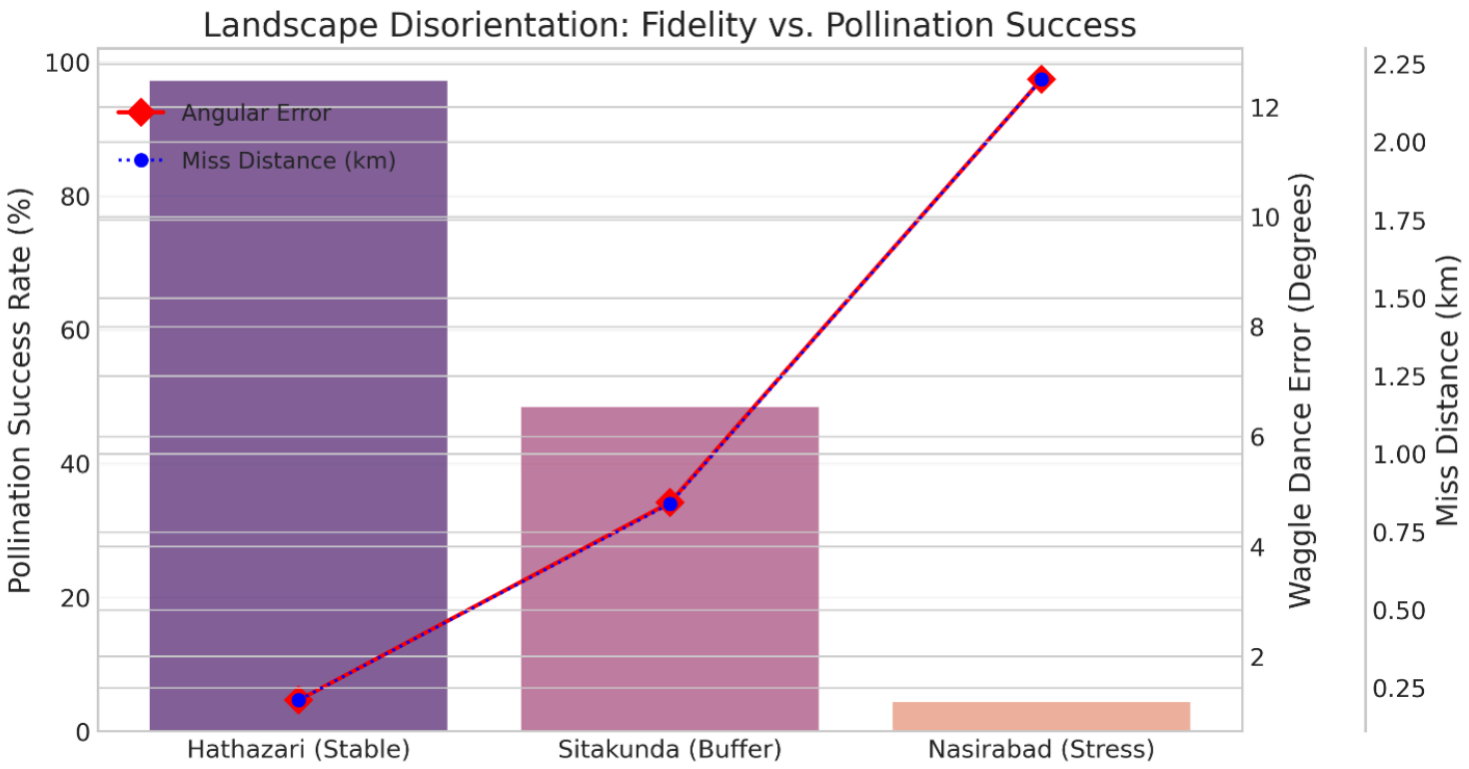



**Figure 6**

**Causal Correlation: Navigational Fidelity vs. Pollination Success**

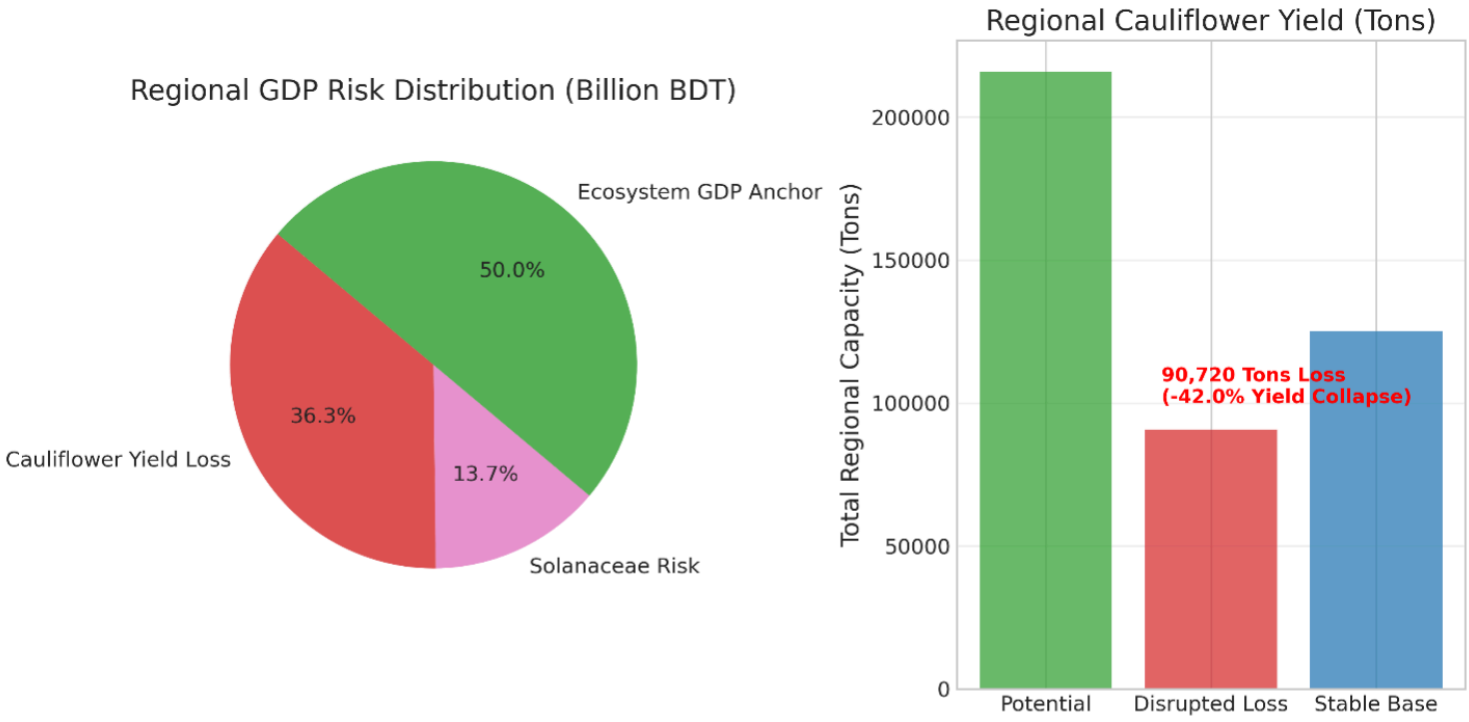



**Figure 7**

**Regional Economic Risk and GDP Vulnerability Profile**

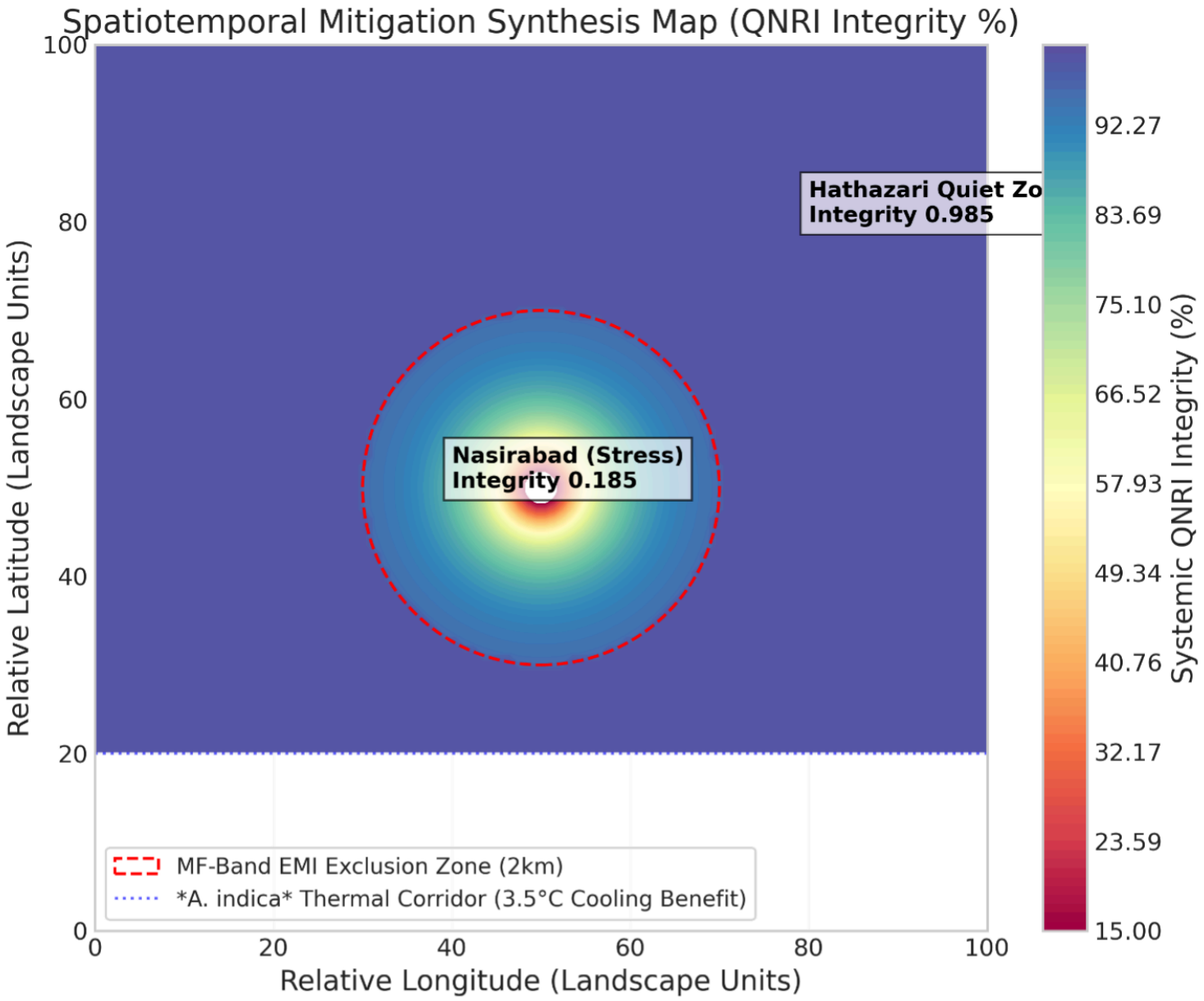



**Figure 8**

**Multiscale Mitigation Synthesis and Buffer Mapping**